

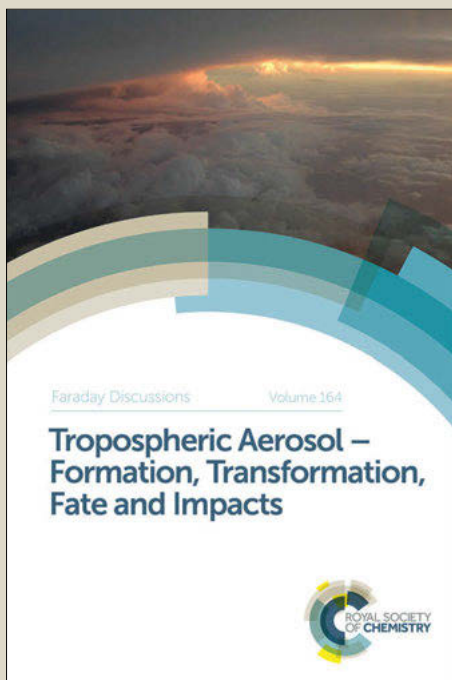
# Faraday Discussions

Accepted Manuscript



This manuscript will be presented and discussed at a forthcoming Faraday Discussion meeting. All delegates can contribute to the discussion which will be included in the final volume.

**Register now to attend!** Full details of all upcoming meetings: <http://rsc.li/fd-upcoming-meetings>



This is an *Accepted Manuscript*, which has been through the Royal Society of Chemistry peer review process and has been accepted for publication.

*Accepted Manuscripts* are published online shortly after acceptance, before technical editing, formatting and proof reading. Using this free service, authors can make their results available to the community, in citable form, before we publish the edited article. We will replace this *Accepted Manuscript* with the edited and formatted *Advance Article* as soon as it is available.

You can find more information about *Accepted Manuscripts* in the [Information for Authors](#).

Please note that technical editing may introduce minor changes to the text and/or graphics, which may alter content. The journal's standard [Terms & Conditions](#) and the [Ethical guidelines](#) still apply. In no event shall the Royal Society of Chemistry be held responsible for any errors or omissions in this *Accepted Manuscript* or any consequences arising from the use of any information it contains.

Cite this: DOI: 10.1039/c0xx00000x

www.rsc.org/xxxxxx

ARTICLE TYPE

## Redox-active electrolyte for supercapacitor application

Elzbieta Frackowiak,\* Mikolaj Meller, Jakub Menzel, Dominika Gastol and Krzysztof Fic

Received (in XXX, XXX) Xth XXXXXXXXX 20XX, Accepted Xth XXXXXXXXX 20XX

DOI: 10.1039/b000000x

5 This paper reports electrochemical behaviour of supercapacitor carbon electrodes operating in different aqueous solutions modified by various redox-active species (hydroxybenzenes, bromine derivatives and iodide). Three dihydroxybenzenes with various stereochemistry, i.e., -OH substitution, have been considered as electrolyte additives ( $0.38 \text{ mol L}^{-1}$ ) in acidic, alkaline and neutral solutions. High capacitance values have been obtained especially for the acidic and alkaline solutions containing 1,4-dihydroxybenzene (hydroquinone). Bromine derivatives of dihydroxybenzenes were also considered as the additive in alkaline solution as the supercapacitor electrolyte and the significant increase of capacitance value was observed. The next investigated redox couple was iodide/iodine system, where  $2 \text{ mol L}^{-1}$  NaI aqueous electrolyte was utilized. In this case the most promising faradaic contribution was achieved during the capacitor operation. Especially, stable capacitance values from  $300\text{--}400 \text{ F g}^{-1}$  have been confirmed by long-term galvanostatic cycling (over 100 000 cycles), cycling voltammetry and floating. The mechanism of pseudocapacitance phenomena was discussed and supported by electrochemical and physicochemical measurements, e.g., *in situ* Raman spectroscopy.

### Introduction

Electrical double layer capacitors (EDLCs) have attracted recently great attention because of their high power rates and excellent cyclability. Total charge accumulated on an electrode/electrolyte interface is proportional to electrochemically available surface area of the electrode, hence, only materials with well developed porosity like activated carbons can play a perfect role as electrode for these devices<sup>[1,2]</sup>. Generally, the capacitance of electrical double layer does not exceed  $120\text{--}150 \text{ F g}^{-1}$  which results in poor energy density, especially in aqueous medium with voltage window limited by water decomposition to *ca.*  $1 \text{ V}$ <sup>[3]</sup>. Obviously, in aprotic organic medium or ionic liquids with the voltage window above  $2.0 \text{ V}$  energy density is significantly higher, but these electrolytes are rather environmentally unfriendly and require expensive assembling process which adversely affects their final price on the market. Apart from charge accumulation in EDL, additional capacitance can be provided from faradaic reactions occurring on the electrode/electrolyte interface<sup>[4]</sup>. Transition metal oxides in symmetric and asymmetric configurations, nitrogen or oxygen enriched carbons with tailored functionalities or electrochemically conducting polymers are usually used for such capacitance enhancement<sup>[5-11]</sup>. On the other hand, pseudocapacitance from electrode materials is always limited by slow diffusion and very often moderate electrolyte penetration. From this point of view, the pseudocapacitance originating from redox active electrolyte solution<sup>[12-15]</sup> seems to be more profitable one; electroactivity of iodine/iodide as well as bromine/bromide redox couples stays at the origin of tremendous

capacity values<sup>[16-22]</sup>, however, these systems still need to be optimized and unusual behaviour should be clearly elucidated. Hence,  $\text{I}^{\cdot}/\text{I}_2$  system has been revisited here and investigated by us in detail. Electrolyte with quinone/hydroquinone<sup>[23-25]</sup> or with other benzene derivatives<sup>[26-30]</sup> can also greatly contribute to pseudocapacitance phenomena. Additionally, molecular grafting of quinones cannot be excluded or neglected<sup>[23,26,27,30-32]</sup>. Abundance of dihydroxybenzene isomers encourage us to study more precisely the influence of substituent location (*ortho*, *meta* or *para*) on their electrochemical activity and tentative application as redox active electrolytes for EDLCs in aqueous medium. All these isomers will be called with their common names recommended by IUPAC; 1,4-dihydroxybenzene will be considered as hydroquinone, 1,3-dihydroxybenzene as resorcinol and 1,2-dihydroxybenzene as catechol. The practical application of the redox active species such as hydroxybenzenes, their bromine derivatives as the electrolyte additives and iodides acting as the supercapacitor electrolyte will be discussed.

### Experimental

All electrochemical measurements were made at ambient conditions, i.e. at temperature ranging from  $21^\circ\text{C}$  to  $25^\circ\text{C}$ . Two- and three electrode capacitors were assembled in a Swagelok® system. For acidic medium gold current collectors were used. Stainless steel collectors served in alkaline and neutral media. Each electrode was composed of 85 wt. % of activated carbon, 10 wt. % of poly(vinylidene fluoride) (PVDF Kynar Flex 2801) and 5 wt. % of carbon black. Microporous carbon prepared by KOH activation<sup>[33]</sup> with surface area of  $1400 \text{ m}^2 \text{ g}^{-1}$  was used to form pressed pellets ( $9.8\text{--}10.3 \text{ mg}$ ) with a geometric surface area

of 0.785 cm<sup>2</sup> per electrode and thickness of about 0.3 mm. Some electrochemical investigations were conducted on microporous carbon tissue (Kynol®) to eliminate an effect of binder. 1 mol L<sup>-1</sup> aqueous solution of H<sub>2</sub>SO<sub>4</sub> with 1,2- and 1,3- as well as 1,4- dihydroxybenzene addition at concentration of 0.38 mol L<sup>-1</sup> served as the electrolytes. To study the pH effect on electrochemical activity of these species (especially 1,4-dihydroxybenzene), 6 mol L<sup>-1</sup> KOH and 1 mol L<sup>-1</sup> Li<sub>2</sub>SO<sub>4</sub> have been also applied. The electrodes were soaked in the appropriate electrolytes and subjected to electrochemical measurements: cyclic voltammetry (CV) at various scan rates (1 - 20 mV s<sup>-1</sup>), constant current charging/discharging (0.2 - 20 A g<sup>-1</sup>) and electrochemical impedance spectroscopy (EIS) in frequency range 100 kHz - 1 MHz with voltage/potential amplitude ±5 mV. To estimate ageing of capacitor a polarization at constant voltage so called floating was performed according to international standards IEC 62391-1. Every 2 hours of floating galvanostatic testing (2 A g<sup>-1</sup>) was done to measure a capacitance. Additionally, full electrochemical characterization (EIS, CV) was performed. For clarity all values of the capacitance are expressed per one electrode that means for total system the capacitance is 25%. Moreover, physicochemical characterisation of carbon materials before and after electrochemical performance was done in order to confirm assumed grafting of redox species. A potentiometric titration of carbon materials was realized at ambient temperature (25°C) using Titrino 848 instrument (Metrohm®, Switzerland). The procedure of pK<sub>a</sub> distribution and proton binding curve calculation was as follows: firstly, pristine carbon material and carbon electrodes (ca. 10 mg) were stirred during 24 hours in 50 mL of 0.01 mol L<sup>-1</sup> NaNO<sub>3</sub> solution with an ionic strength of 0.01. After stirring, pH of the solution (containing carbon material) was measured and adjusted to 3 by controlled 0.1 mol L<sup>-1</sup> HCl addition. After 15 minutes of pH stabilization, the solution was titrated by 0.1 mol L<sup>-1</sup> NaOH till pH 11. The experimental data were transformed to proton binding isotherms Q(pH) representing total protonated sites. Briefly, proton binding isotherm is closely related with pK<sub>a</sub> distribution by following equation:

$$Q(pH) = \int q(pH, pK_a) \cdot f(pK_a) dpK_a$$

A solution of the equation was attained using the numerical procedure SAIEUS® (Solution of Adsorption Integral Equation Using Splines) by Jacek Jagiello (Micromeritics®, USA).

In order to compare and to confirm the results obtained by the potentiometric titration, TGA experiments were done. All carbon materials were subjected to heating until 950°C with 10 K min<sup>-1</sup> heating rate using 50 mL min<sup>-1</sup> Ar protective flow in Jupiter 209 thermomicrobalance (Netzsch®, Germany). The mass change was recorded simultaneously with mass spectra analysis of decomposition products (done on Aelos instrument by Netzsch®, Germany). Particularly, m/e = 18, 28 and 44 signals were studied, because one can assume that they might be related to H<sub>2</sub>O, CO and CO<sub>2</sub> evolution. Furthermore, these compounds indicate a presence of oxygen functional groups, generated during grafting process.

Apart from dihydroxybenzene also bromine derivatives have

been studied, i.e., dibromodihydroxybenzene as a source of redox reactions in the electrolyte. The amount of the additive was 0.2 mol L<sup>-1</sup> C<sub>6</sub>H<sub>4</sub>Br<sub>2</sub>O<sub>2</sub> dissolved in different concentrations of KOH (1 - 6 mol L<sup>-1</sup>).

To study the effect of halides on the capacitor performance 2 mol L<sup>-1</sup> NaI aqueous solution was used. Such concentration was selected from the previous studies [18]. For careful analysis of the pseudocapacitive effects, *in situ* studies were performed using DXR dispersive Raman microscope Thermo Fischer Scientific (USA) equipped with laser of 532 nm wavelength and 5 mW power; fluorescence and white light linearly corrected, with medium cosmic radiation threshold detection.

## Results and discussion

Detailed electrochemical characterization was realized in order to evaluate electrochemical activity of aforementioned redox active species by various methods.

### Dihydroxybenzenes

Cyclic voltammetry (CV) performed at various scan rates (1 mV s<sup>-1</sup> to 20 mV s<sup>-1</sup>) for dihydroxybenzenes in 1 mol L<sup>-1</sup> H<sub>2</sub>SO<sub>4</sub> revealed strong influence of hydroxyl group location on their electrochemical activity. CV curves at 10 mV s<sup>-1</sup> with measured current values recalculated to capacitance are presented in Fig. 1.

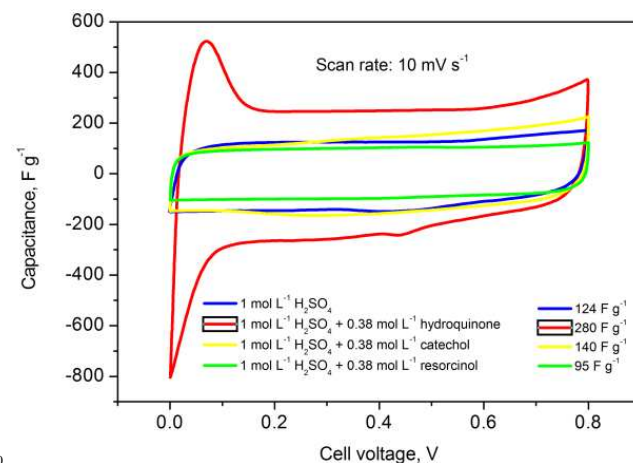
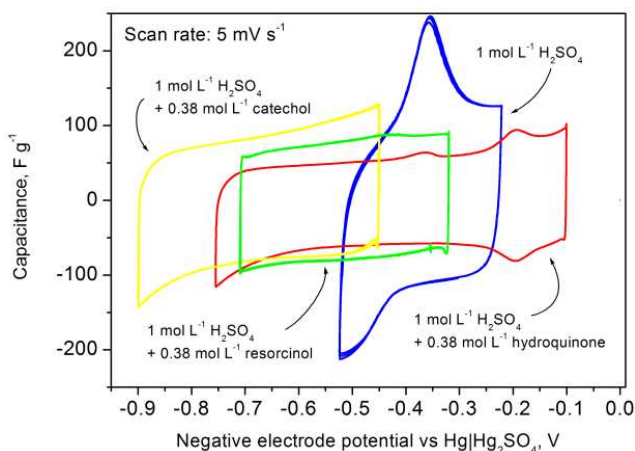


Fig. 1 Cyclic voltammograms for capacitors operating in 1 mol L<sup>-1</sup> H<sub>2</sub>SO<sub>4</sub> solution with different dihydroxybenzenes

Capacitor operating in pure 1 mol L<sup>-1</sup> H<sub>2</sub>SO<sub>4</sub> solution is also shown for comparison. The highest capacitance values were observed for the capacitor operating in 1 mol L<sup>-1</sup> H<sub>2</sub>SO<sub>4</sub> with 0.38 mol L<sup>-1</sup> hydroquinone, i.e. 280 F g<sup>-1</sup> in comparison to 124 F g<sup>-1</sup> for the electrolyte without hydroquinone. For capacitor operating in the electrolyte with catechol addition an increase of capacitance is rather insignificant (140 F g<sup>-1</sup>) and for the electrolyte with resorcinol the capacitance is even worse than for an unmodified 1 mol L<sup>-1</sup> H<sub>2</sub>SO<sub>4</sub> (95 F g<sup>-1</sup>). It might be related to worse conductivity of the electrolyte solution, aggravated by resorcinol addition as well as with some pore blocking. More detailed information was obtained from a three-electrode cell.

Cyclic voltammograms (5 mV s<sup>-1</sup>) for negative and positive electrode separately are provided in Figs. 2 and 3.



**Fig. 2** Cyclic voltammograms for negative electrode at  $5 \text{ mV s}^{-1}$  scan rate operating in dihydroxybenzene-modified acidic electrolytes

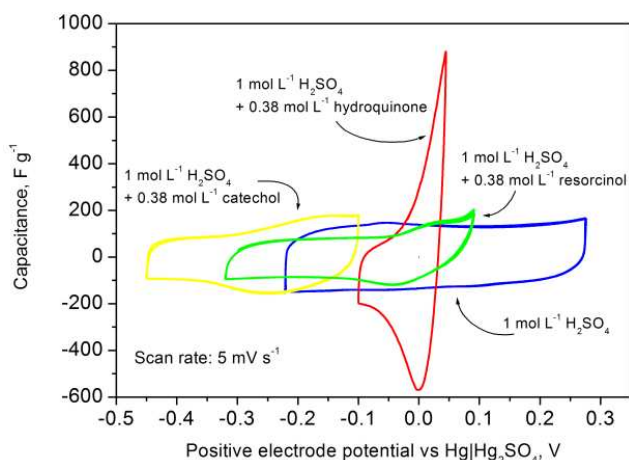


**Fig. 3** Cyclic voltammograms for positive electrode at  $5 \text{ mV s}^{-1}$  scan rate operating in dihydroxybenzene-modified acidic electrolytes

Both electrodes have different electrochemical response and they operate at a significantly shifted range of potential even if capacitor works at constant voltage ( $0.8 \text{ V}$ ) and the same pH. These results are in good agreement with the values obtained in the two-electrode cell. Typical redox behaviour with a sharp peak can be observed especially for the electrolyte containing  $0.38 \text{ mol L}^{-1}$  of hydroquinone. Apart from characteristic reduction/oxidation of these species (immobilized on positive electrode) disclosed by high capacitance values in very narrow potential range (only  $100 \text{ mV}$ ), hydroquinones can be also electrochemically "grafted" onto carbon surface being an additional source of pseudocapacitance. Such electrochemical "grafting" is presented in Fig. 4 where total capacitance of a system operating in  $1 \text{ mol L}^{-1} \text{ H}_2\text{SO}_4$  with  $0.38 \text{ mol L}^{-1}$  hydroquinone increases with a cycle number. It confirms that quinone-hydroquinone functionalities can be "grafted" and/or strongly attracted through  $\pi$  bonding on the carbon surface without aggravating conductivity of the electrode. The capacitance originated only from electrostatic attraction of ions in sulphuric acid solution was equal to ca.  $125 \text{ F g}^{-1}$  for the first cycles; after 550 cycles total capacitance was  $283 \text{ F g}^{-1}$ . It clearly suggests a faradaic origin of the capacitance increase.

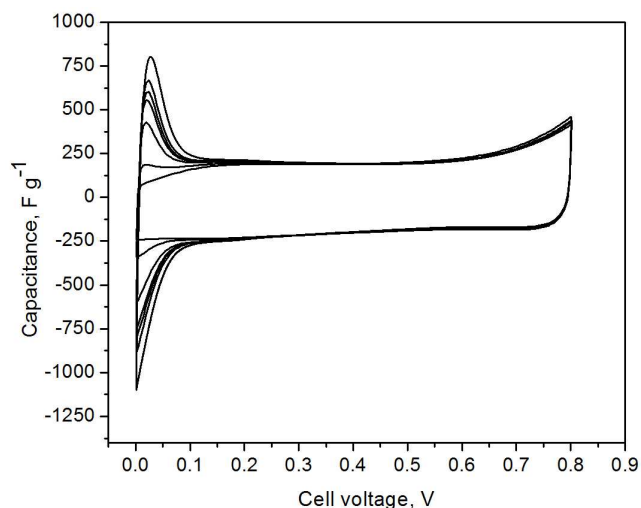


**Fig. 4** Cyclic voltammogram ( $5 \text{ mV s}^{-1}$ ) for capacitor operating in  $1 \text{ mol L}^{-1} \text{ H}_2\text{SO}_4$  with  $0.38 \text{ mol L}^{-1}$  hydroquinone additive

Unfortunately, it is impossible to determine precisely a contribution of a charge provided by simple reduction and oxidation of immobilized hydroquinone on the electrode/electrolyte interface and charge provided by redox activity of quinone-type functionalities bonded to the surface.

A big discrepancy between behaviour of positive and negative electrode is also well observed during galvanostatic charge-discharge investigation at current load of  $0.5 \text{ A g}^{-1}$  (Fig. 5). Positive electrode operates at  $0.1 \text{ V}$  potential range. Unfortunately, an efficiency of this process is quite low ( $63\%$ ) that proves its high irreversibility, hence, practical application of this redox couple could be limited.

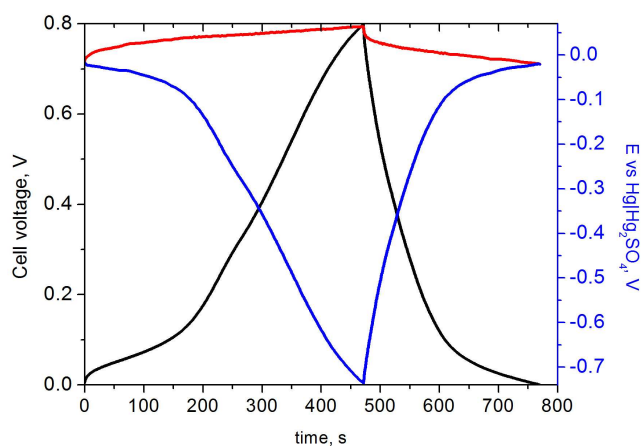


**Fig. 5** Galvanostatic charging/discharging curve at current load of  $0.5 \text{ A g}^{-1}$  for capacitor operating in  $1 \text{ mol L}^{-1} \text{ H}_2\text{SO}_4$  with  $0.38 \text{ mol L}^{-1}$  hydroquinone additive

Electrochemical impedance spectroscopy results also follow a tendency observed for cyclic voltammetry and galvanostatic charging/discharging. Tremendous capacitance values revealed by the electrodes operating in  $1 \text{ mol L}^{-1} \text{ H}_2\text{SO}_4$  with  $0.38 \text{ mol L}^{-1}$  hydroquinone are assumed to be attributed to redox process of quinone/hydroquinone couple; high capacitance values (even ca.  $1500 \text{ F g}^{-1}$  at  $1 \text{ mHz}$ ) recorded only at low frequency regimes were accompanied by moderate charge propagation, which implies diffusion-limited process contributing in a charge

accumulation. Obviously such high capacitance values will never have practical application. At high frequencies no significant difference in electrochemical behaviour was observed; the results in form of Nyquist and Bode plots are presented in Figs. 6-8.

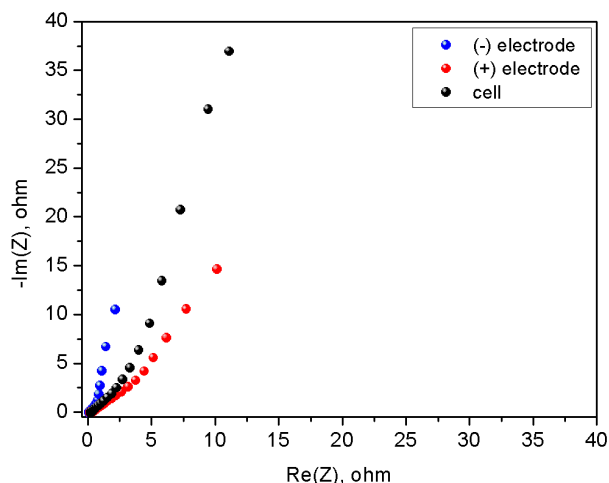


Fig. 6 Nyquist plot for capacitor operating in 1 mol L<sup>-1</sup> H<sub>2</sub>SO<sub>4</sub> with 0.38 mol L<sup>-1</sup> hydroquinone additive

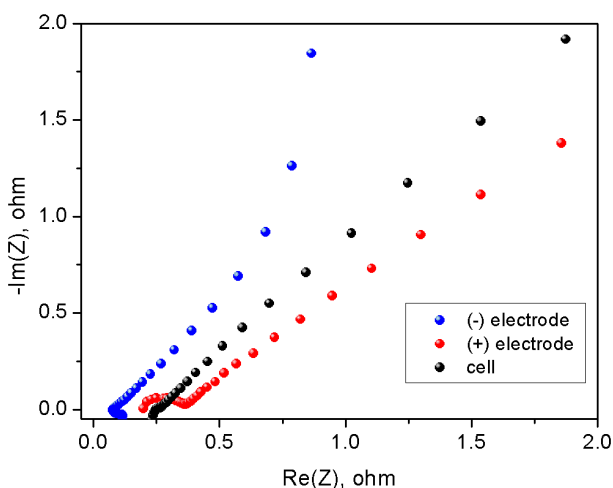


Fig. 7 Low frequency inset of Nyquist plot for capacitor operating in 1 mol L<sup>-1</sup> H<sub>2</sub>SO<sub>4</sub> with 0.38 mol L<sup>-1</sup> hydroquinone additive

For positive electrode operating in 1 mol L<sup>-1</sup> H<sub>2</sub>SO<sub>4</sub> with 0.38 mol L<sup>-1</sup> hydroquinone additive, a typical faradaic response was observed; it suggests that this electrode is mainly responsible for redox contribution in the system (Fig. 7).

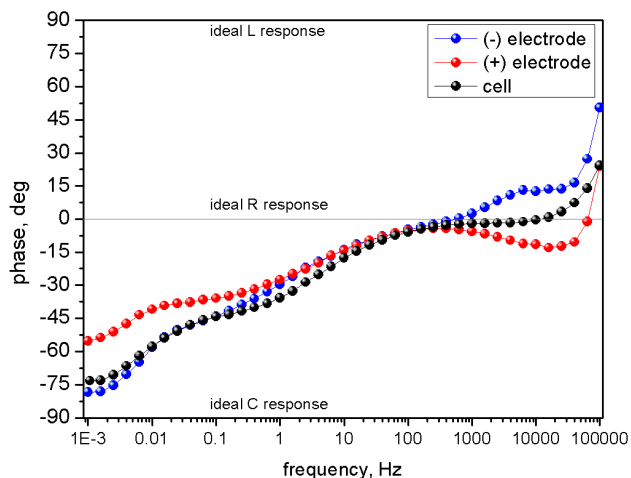


Fig. 8 Bode plot for capacitor operating in 1 mol L<sup>-1</sup> H<sub>2</sub>SO<sub>4</sub> with 0.38 mol L<sup>-1</sup> hydroquinone additive

The change of phase angle (Fig. 8) also suggests different type of charge storage mechanisms, especially in diffusion limited area, i.e., in low frequency region. For negative electrode, the course is rather monotonic and confirms rather electrostatic type of charge accumulation. On the other hand, two humps observed for positive electrode suggest the combination of the typical faradaic and electrostatic (capacitive) processes.

The impedance spectra for the capacitors operating in various dihydroxybenzenes dissolved in 1 mol L<sup>-1</sup> H<sub>2</sub>SO<sub>4</sub> aqueous solution are presented in Fig. 9.

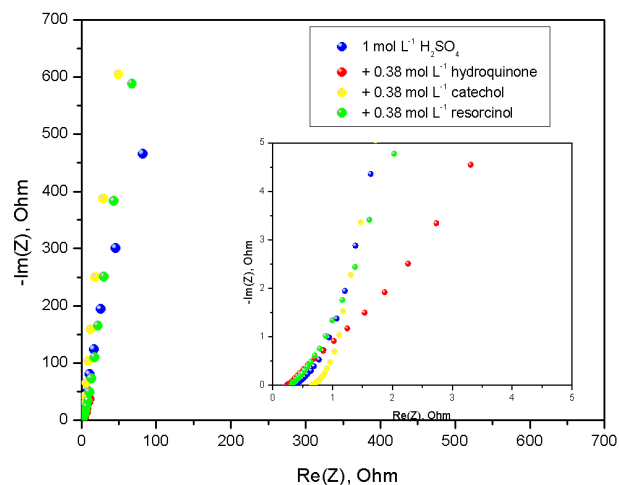
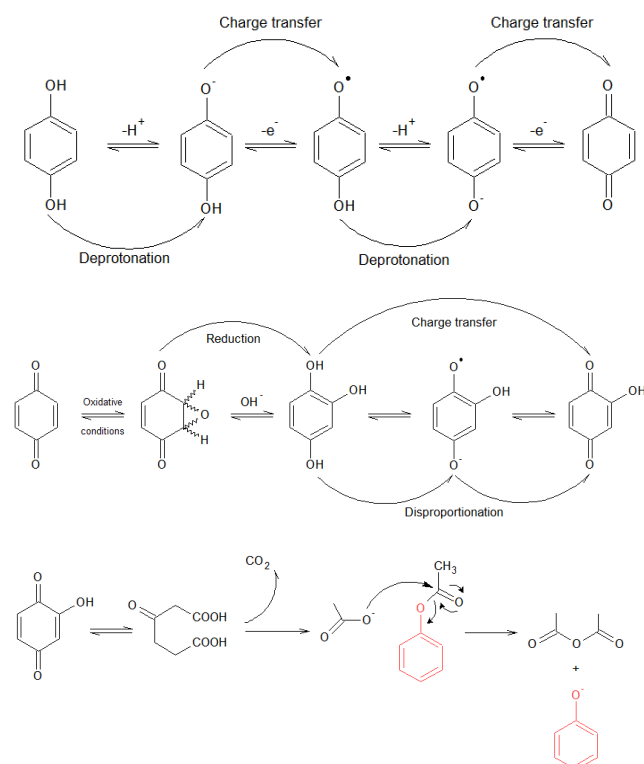


Fig. 9 Nyquist plots for capacitors operating in 1 mol L<sup>-1</sup> H<sub>2</sub>SO<sub>4</sub> with 0.38 mol L<sup>-1</sup> dihydroxybenzene additives

As it can be seen in Figs. 2, 3 and 10, electrochemical activity of dihydroxybenzenes strongly depends on hydroxyl group location (*para*, *ortho* or *meta*). In acidic medium hydroquinone with *para*-type substitution is the most active because of a distance between hydroxyl groups in benzene ring. Electrochemical activity of quinone/hydroquinone redox couple is presented in Fig. 10. In case of catechol, hydroxyl groups can be oxidized even with aromatic structure deformation but this process does not occur so easily as for hydroquinones. Resorcinol oxidation requires an additional activator in a reaction medium because the oxidized form of this compound contains unstable and thermodynamically non-preferable conjunction of *meta*-benzoquinone bonds, so its

oxidation was not observed.



5 **Fig. 10** Electrochemical activity of hydrobenzenes in aqueous electrolytic medium on activated carbon electrodes

Additionally, the substituent location (*para*, *ortho* or *meta*) strongly affects the electrode potential range. Significant shifts towards more cathodic values were recorded for catechol (-400 mV) and resorcinol (-200 mV). On the other hand, the potential range for positive electrodes operating in these electrolytes are narrower which implies their faradaic activity, especially for the electrolyte with hydroquinone. Obviously, reduction/oxidation processes on activated carbon electrodes cannot follow straightforwardly Nernstian manner with well-defined peaks because on these electrodes diffusion strongly affects the transport from electrolyte bulk to electrode surface which results in an ill-defined potential wave. Moreover, considering the fact that quinone reduction/oxidation is a proton consuming-process, the electrochemical activity should also depend strongly on the pH of the electrolyte. In order to investigate an influence of the pH, three most often applied electrolytes, i.e., 1 mol L<sup>-1</sup> H<sub>2</sub>SO<sub>4</sub>, 1 mol L<sup>-1</sup> Li<sub>2</sub>SO<sub>4</sub> and 6 mol L<sup>-1</sup> KOH were selected and modified by a hydroquinone addition (0.38 mol L<sup>-1</sup>). Cyclic voltammograms recorded at 10 mV s<sup>-1</sup> scan rate are presented in Fig. 11.

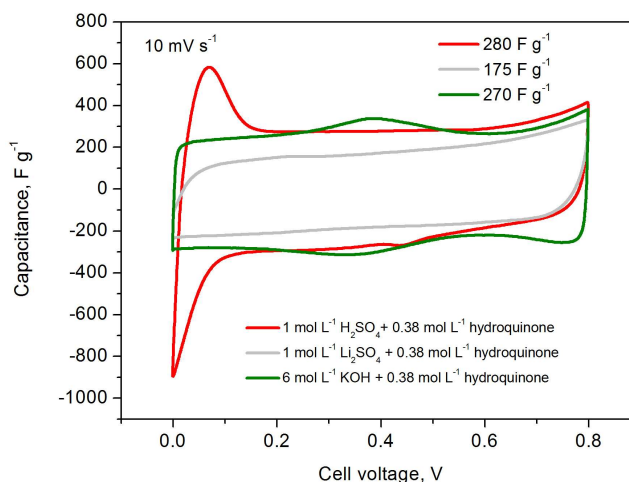


**Fig. 11** Cyclic voltammograms for capacitor operating in aqueous electrolytes of different pH with hydroquinone addition

30 The capacitance values are significantly higher for the capacitor operating in alkaline and acidic media (i.e., 283 and 275 F g<sup>-1</sup>, respectively) than for the neutral one (140 F g<sup>-1</sup>). Additionally, obtained capacitance values are considerably higher than for the capacitors operating in unmodified electrolytes; for the capacitor, operating in 6 mol L<sup>-1</sup> KOH electrolyte, measured capacitance at the same scan rate was ca. 130 F g<sup>-1</sup>, for 1 mol L<sup>-1</sup> H<sub>2</sub>SO<sub>4</sub> it was 123 F g<sup>-1</sup>; for Li<sub>2</sub>SO<sub>4</sub> solution, no significant difference in the capacitance was observed. Moreover, the different shape of cyclic voltammograms for the capacitors operating in acidic and alkaline media implies different quinone|hydroquinone reduction and oxidation mechanism. In acidic medium with readily accessible protons these processes occur quite easily along applied voltage. In alkaline medium strong intermolecular hydrogen-bonding interactions between quinone and the hydroxyl and functional groups have a significant influence on redox kinetics, therefore, their activity can be observed in the narrow voltage range disclosed as small but reversible peaks. Three-electrode investigation confirmed that neither well-defined redox response is on positive nor negative electrode, however, an increase of their capacitance have been observed (Fig. 12).

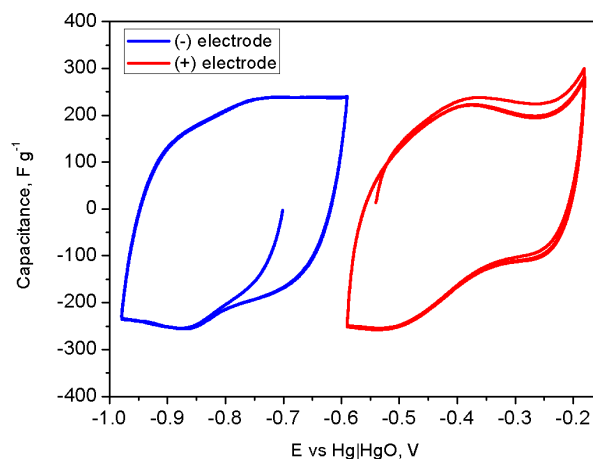


**Fig. 12** Cyclic voltammograms for positive and negative electrode of capacitor operating in 6 mol L<sup>-1</sup> KOH with hydroquinone addition

Galvanostatic charge/discharge also confirms that in alkaline medium no typical redox response could be observed. Two- and three- electrode investigation at  $0.5 \text{ A g}^{-1}$  is presented in Fig. 12.

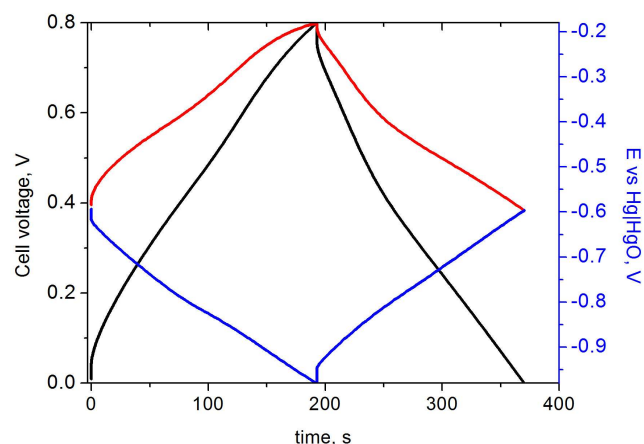
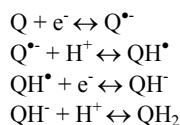
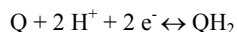


Fig. 13 Galvanostatic charging/discharging curve at current load of  $0.5 \text{ A g}^{-1}$  for capacitor operating in  $6 \text{ mol L}^{-1} \text{ KOH}$  with  $0.38 \text{ mol L}^{-1}$  hydroquinone additive

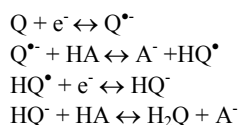
Finally, redox activity of quinone (Q) | hydroquinone ( $\text{QH}_2$ ) redox couple can be described by the following reactions in acidic medium:



giving finally:



and without proton in alkaline (HA) medium:



giving finally:



Additionally, self-protonation cannot be neglected.

Physicochemical measurements of the both electrodes conducted separately after electrochemical polarization in the presence of  $\text{H}_2\text{Q}$  in acidic medium are also in good accordance with the results obtained from the electrochemical investigation. Proton binding curves, revealed higher oxygen-based functionalities on carbon electrodes, especially in range of  $\text{pK}_a$  related with  $=\text{CO}$  functional groups (i.e. in range 8-9) or for easily protonated ones with  $\text{pK}_a$  close to 5. Unfortunately, with a sensitivity of the method, one cannot determine precisely the type of functionalities, even if in the literature some assumptions are

presented. Especially for the peaks in  $\text{pK}_a$  range 8.5 – 10.0 one can observe some difference in response, however, they are too close to each other to differentiate them and attribute to typical functional groups. The most intensive peaks observed at the  $\text{pK}_a$  3 and 11 should be related to buffering effect of water.

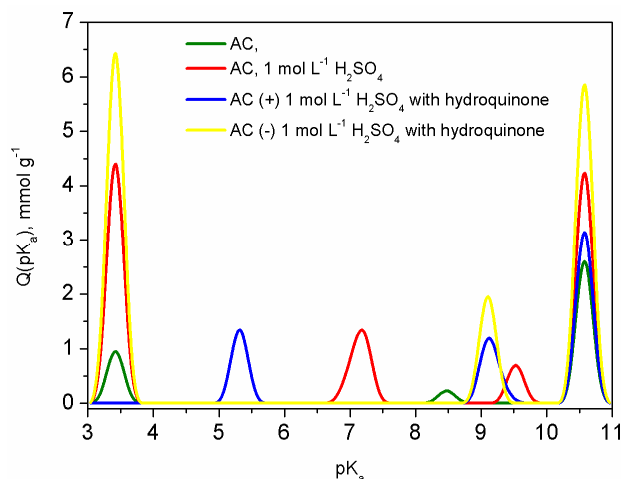


Fig. 14 Proton-binding curves for activated carbons

TGA-MS experiments gave even more reliable evidence for increase of oxygen-based functionalities. The mass change of the activated carbon, subjected to the investigation and serving as a reference, was 7%. For the electrode after operation in the unmodified  $1 \text{ mol L}^{-1} \text{ H}_2\text{SO}_4$ , the mass change was 24%, with a significant decomposition signal of  $m/e=44$  at  $200\text{-}300^\circ\text{C}$ , which suggests the evacuation of carboxyl-like functional groups. The mass change of the electrode after electrochemical operation in electrolyte containing  $0.38 \text{ mol L}^{-1}$  of hydroquinone is slightly lower, i.e. 23%, which suggests slower decomposition of generated species. Especially, the significant increase of  $m/e=28$  signal, related to  $=\text{CO}$  functional groups, decomposing at higher temperatures was observed. It suggests that instead of carboxyl-like functionalities, some carbonyl species were generated. For negative electrode of the capacitor operating in  $1 \text{ mol L}^{-1} \text{ H}_2\text{SO}_4$  containing  $0.38 \text{ mol L}^{-1}$  of hydroquinone, the recorded mass change was 26%. The kinetics of decomposition in this case suggests the major contribution of fast evacuation of carboxyl-like functionalities, with some carbonyl-like species evacuating slowly at higher temperatures.

#### Redox activity of dibromodihydroxybenzene

Apart from pure dihydroxybenzenes as the additives to electrolyte, their bromine derivative such as  $\text{C}_6\text{H}_4\text{Br}_2\text{O}_2$  has been used as the redox active species. The same microporous powdered carbon was used for the electrode preparation in our investigations.  $\text{C}_6\text{H}_4\text{Br}_2\text{O}_2$  compound was soluble only in KOH medium. Therefore, different concentrations of the solvent (KOH) varying from 1 to  $6 \text{ mol L}^{-1}$  were applied in order to determine the optimal operating condition of the system. It was found that a capacitor operation in  $2 \text{ mol L}^{-1} \text{ KOH}$  resulted in the highest values of capacitance, i.e. about  $270 \text{ F g}^{-1}$  from cyclic voltammetry and galvanostatic cycling ( $318 \text{ F g}^{-1}$  from electrochemical impedance spectroscopy). It was also confirmed that the capacitor incorporating  $0.2 \text{ mol L}^{-1} \text{ C}_6\text{H}_4\text{Br}_2\text{O}_2 + 2 \text{ mol L}^{-1}$

<sup>1</sup> KOH exhibits the highest capacitance in comparison with 2 mol L<sup>-1</sup> KOH and 0.2 mol L<sup>-1</sup> C<sub>6</sub>H<sub>6</sub>O<sub>2</sub> + 2 mol L<sup>-1</sup> KOH, Figs.15,16.

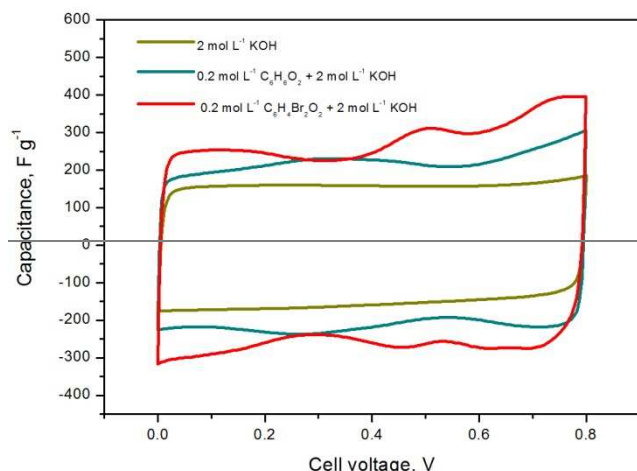


**Fig. 15** Capacitance vs. voltage of the systems operating in 2 mol L<sup>-1</sup> KOH with 0.2 mol L<sup>-1</sup> C<sub>6</sub>H<sub>6</sub>O<sub>2</sub> and 0.2 mol L<sup>-1</sup> C<sub>6</sub>H<sub>4</sub>Br<sub>2</sub>O<sub>2</sub>

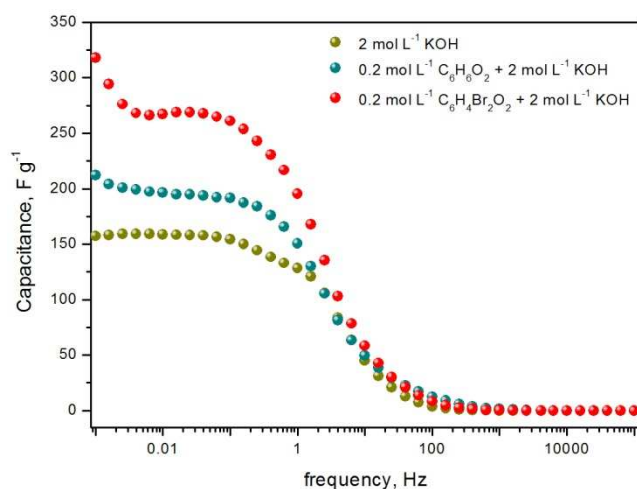


**Fig. 16** Capacitance vs. frequency of the systems operating in 2 mol L<sup>-1</sup> KOH with 0.2 mol L<sup>-1</sup> C<sub>6</sub>H<sub>6</sub>O<sub>2</sub> and 0.2 mol L<sup>-1</sup> C<sub>6</sub>H<sub>4</sub>Br<sub>2</sub>O<sub>2</sub>

The best capacitance performance was also noted in case of the investigated compound in 2 mol L<sup>-1</sup> KOH during the galvanostatic charging/discharging technique (2 A g<sup>-1</sup>) reaching the value of about 255 F g<sup>-1</sup> and resulting in 17% capacitance decay after 5000 cycles. The capacitance enhancement noted for the system with the bromide compound results from the substitution reactions between Br<sup>-</sup> in aromatic ring and OH<sup>-</sup> species present in alkaline solution; these reactions might additionally contribute to total capacitance obtained. Because of strong alkaline pH, reactions of Br<sup>-</sup>/BrO<sub>3</sub><sup>-</sup> play rather minor role, but cannot be neglected. A presence of Br<sup>-</sup> ions slightly shifts the potential of quinone/hydroquinone redox couple (ca. 150 mV), hence, the capacitance is achieved at higher voltage values. Moreover, substitution of Br<sup>-</sup> by OH<sup>-</sup> group results in another source for pseudocapacitance, because *p*-dihydroxybenzene becomes trihydroxybenzene with two active configurations of OH<sup>-</sup> group: two in *p*-position and two in *o*-position, able to undergo redox reaction within hydroquinone/quinone couple.

#### Iodide as redox active species

Our previous studies [16-18] on iodide for capacitor application have been focused on electrochemical characterization and physicochemical properties of electrolytic solutions as well as determination of a role of cation. Presently special attention was devoted to a long-term cycling of sodium iodide aqueous solution as the electrolyte of the capacitor. 2 mol L<sup>-1</sup> NaI solution exhibited good conductivity value of 275 mS cm<sup>-1</sup>. Floating was selected as the most destructive method for evaluation of cycle life of the capacitor. The capacitor was constantly polarized at 1.2V for 200 hours. During this time it was regularly tested by cyclic voltammetry, galvanostatic charge/discharge and electrochemical impedance spectroscopy to estimate its state of health. Capacitance *versus* floating time (Fig. 17) indicates unusual capacitance enhancement with subsequent cycles. However, detailed analysis of this phenomenon shows how careful but also critical evaluation of data is necessary. For example, even if galvanostatic method is considered as the most adapted for capacitance estimation, slightly various values can be obtained from various formulas for C (considering total discharge time or typical slope from galvanostatic discharge curve).

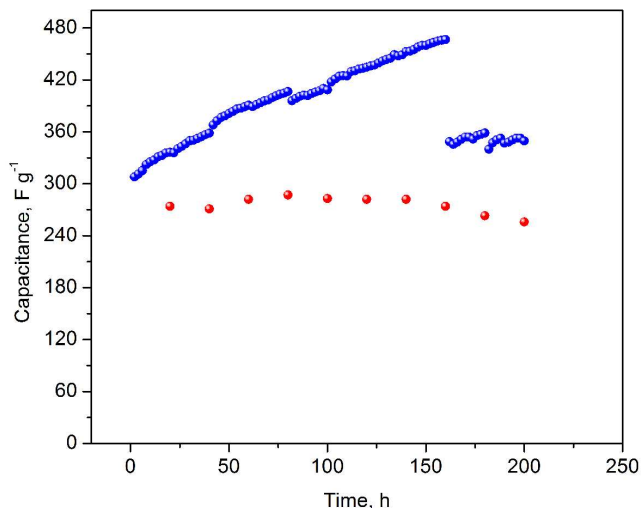


**Fig. 17** Capacitance vs. floating time for capacitor operating in 2 mol L<sup>-1</sup> NaI solution (capacitance calculated from two different formulas)

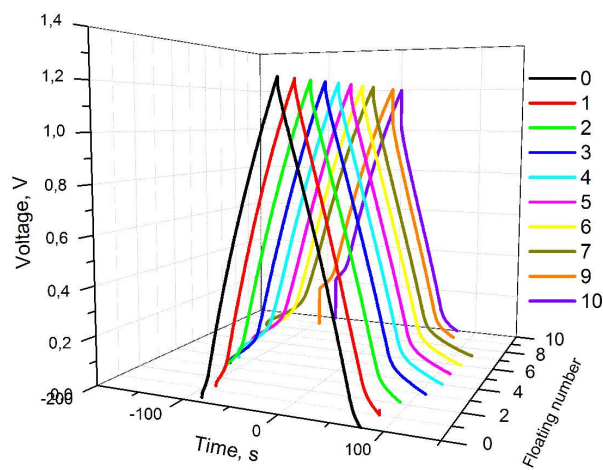


**Fig. 18** Charge/discharge profiles for  $2 \text{ A g}^{-1}$  current load vs. floating time for  $2 \text{ mol L}^{-1}$  NaI solution

Taking into account full time of the capacitor discharging at current load of  $2 \text{ A g}^{-1}$  (Fig. 18) the higher capacitance values are obtained than calculated from a slope of the galvanostatic discharge characteristics (blue points in Fig. 17). Capacitance calculated from the slope as a function of floating time (red points in Fig. 17) does not show a great tendency of growth but it is extremely stable (varying from  $250$  to  $280 \text{ F g}^{-1}$  at  $2 \text{ A g}^{-1}$ ). This enormous capacitance increase during floating has been also monitored by cyclic voltammetry at  $5 \text{ mV s}^{-1}$  (Fig. 19) as well as by electrochemical impedance spectroscopy (Fig. 20).

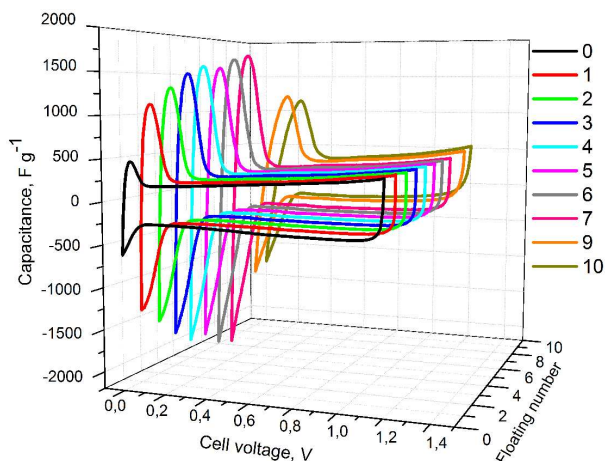


**Fig. 19** Capacitance from cyclic voltammetry ( $5 \text{ mV s}^{-1}$ ) vs. floating time for  $2 \text{ mol L}^{-1}$  NaI solution

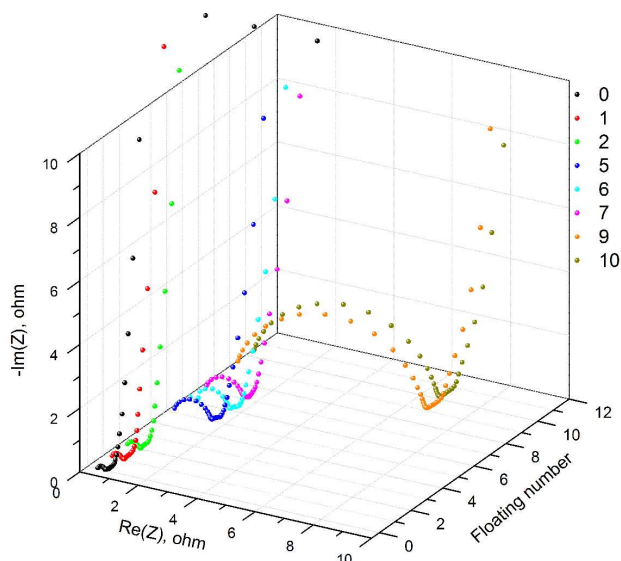


**Fig. 20** Nyquist impedance spectra recorded after several floating tests for capacitor in  $2 \text{ mol L}^{-1}$  NaI solution

The gradual capacitance increase on the voltammetry characteristics in the narrow range of voltage (Fig. 19) matches very well with the charge transfer increase in Fig. 20 that reflects participation of redox reactions. It is noteworthy that the equivalent series resistance (ESR) is extremely small ( $0.3 \text{ ohm}$ ) and very stable during all floating time. Contrarily resistance  $R_{CT}$

gradually increases from negligible values to  $6 \text{ ohm}$  after floating. Our experiments proved that  $200$  hours of floating at  $1.2 \text{ V}$  was equivalent to more than  $110\,000$  galvanostatic cycles at  $1 \text{ A g}^{-1}$ . After this long-term galvanostatic cycling  $91\%$  capacitance retention was still preserved.

Regardless of the testing method (floating or galvanostatic charge/discharge) no corrosion was observed on the stainless steel current collectors that is an additional benefit in practical application. Moreover, this halide is more environmentally friendly than bromine.

For elucidation of charge storage mechanism of iodide solutions *in situ* Raman spectroscopy method was used. Briefly, D and G band ratio (Raman shift of  $1333$  and  $1597 \text{ cm}^{-1}$ , respectively) for our activated carbon material was equal to  $1.05$ , i.e., typical for this type of disordered material. Shape of ill-defined, broad D band confirms expected distortions of carbon network, being namely more benzenoid than graphitic (graphene-like). Moreover, two-component G-band (at Raman shift close to  $E_{2g2}$  mode,  $\sim 1580 \text{ cm}^{-1}$ ), suggests various interaction between vibrational C-C covalent bonds within the aromatic plane with various length and strength which is considered as typical for disordered, activated carbons.

Carbon microelectrode (geometric area of  $0.283 \text{ cm}^2$ ) made from AC powder as well in the form of tissue placed on the gold support was polarized by cyclic voltammetry in the range from  $0$  till  $750 \text{ mV vs. SCE}$  and potentiostatically from OCP (ca.  $240 \text{ mV vs. SCE}$ ) till  $750 \text{ mV vs. SCE}$  with  $50 \text{ mV}$  potential stepwise. The cyclic voltammetry demonstrated a typical capacitive behaviour of the electrode in a potential range up to  $550 \text{ mV vs. SCE}$  and a significant increase of measured current above  $600 \text{ mV vs. SCE}$ , related with iodide/iodine redox couple activity. It has to be noticed that spectra recorded in the potentiostatic mode were collected after ca.  $5$  minutes of potential polarization, i.e. when the current response was stable. The current recorded in EDL charging area was of  $\sim 95 \mu\text{A cm}^{-2}$ , whereas for redox activity region this value increased to  $\sim 330 \mu\text{A cm}^{-2}$ .

D/G ratio and their Raman shift did not change remarkably with the polarization of the carbon in the iodide solution, however, for the longer polarization at  $750 \text{ mV vs. SCE}$  a small shift of  $3 \text{ cm}^{-1}$  was observed, especially for D band. On the other hand, spectra in the low wavelength range were drastically modified by the polarization in the iodide electrolyte, with a remarkable increase of the  $I_3^-$  signal with polarization time. Raman spectra recorded at potentiostatic mode are shown in Fig. 21.

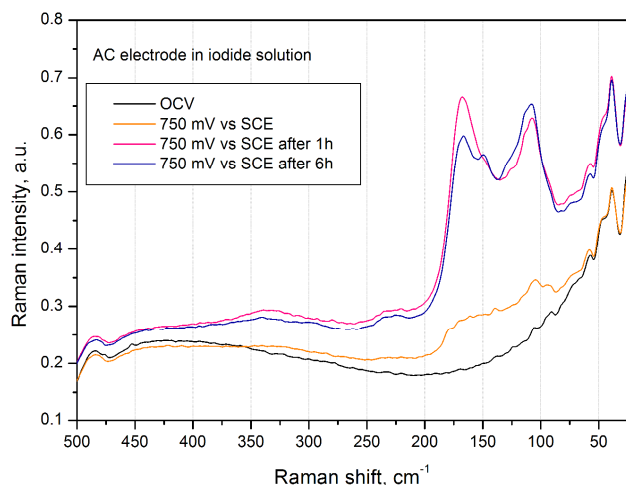


**Fig. 21** Raman spectra recorded *in-situ* for activated carbon fabric in 2 mol L<sup>-1</sup> NaI during potentiostatic polarization

Considering the profiles of recorded spectra, we propose following mechanism. Firstly, I<sup>-</sup> is oxidized to I<sub>2</sub> giving various broad bands in the Raman shift region of 190-170 cm<sup>-1</sup> (for pure iodine 179 cm<sup>-1</sup>). Iodine dissolved in electrolyte solution might recombine with monoiodide I<sup>-</sup> resulting in I<sub>3</sub><sup>-</sup> species [34-35]. It is clearly seen that complex I<sub>3</sub><sup>-</sup> is formed from I<sub>2</sub>·I<sup>-</sup> complex, enforcing 168 cm<sup>-1</sup> vibrational response. As expected, the Raman intensity increases in time, hence, one can assume that the concentration of I<sub>3</sub><sup>-</sup> species increases and their presence affects the Raman spectra profile quantitatively. Moreover, another peak at 108 cm<sup>-1</sup> appears and can be attributed to I<sub>5</sub><sup>-</sup> complex. It has to be noticed that I<sub>5</sub><sup>-</sup> consists of I<sub>2</sub> and I<sub>3</sub><sup>-</sup> species, hence, their Raman activity is observed simultaneously. However, for a longer polarization time, the major contribution of I<sub>3</sub><sup>-</sup> in the profile decreases, hence, a recombination of I<sub>2</sub> towards polyiodides as I<sub>5</sub><sup>-</sup> is observed. I<sub>5</sub><sup>-</sup> starts to contribute in the spectra even after 1h of the polarization, with a small signal at 150 cm<sup>-1</sup>, enforced significantly after 6hrs of the polarisation and recognized for bent C<sub>2v</sub> modes of chained, discrete I<sub>5</sub><sup>-</sup>. One can expect that the response at 368-270 cm<sup>-1</sup> and 268-214 cm<sup>-1</sup> can be ascribed to iodine in the molecular form but also to C-I interactions. Especially, signal recorded at 333 cm<sup>-1</sup> and 327 cm<sup>-1</sup> might be considered as C-I<sub>3</sub><sup>-</sup> and C-I<sub>5</sub><sup>-</sup> bands, respectively, but their presence at lower Raman shifts (e.g. 165 and 115 cm<sup>-1</sup>) cannot be directly confirmed because of strong activity of pure I<sub>3</sub><sup>-</sup> and I<sub>5</sub><sup>-</sup> bands. Generally, all forms of iodides present in the electrolyte solution and at the electrode/electrolyte interface reflect complex Raman signal as a combination of major I<sub>2</sub> and I<sub>n</sub><sup>-</sup> bands and an interaction between the bands in I<sub>2</sub> molecule and related species [35-37]. Even if the *in situ* Raman experimental conditions are quite far from real capacitor operation, this technique supplies important information on this peculiar carbon/iodine interface.

## Conclusions

Electrochemical behaviour of carbon-based electrochemical capacitors operating in different redox active solutions has been reported. The dihydroxybenzenes with various -OH substitution

(*ortho*, *meta*, *para*) as additives (0.38 mol L<sup>-1</sup>) to various aqueous electrolytes were serving as the source of pseudocapacitance. The highest capacitance values (283 F g<sup>-1</sup> at 5 mV s<sup>-1</sup>) were observed for 0.38 mol L<sup>-1</sup> hydroquinone dissolved in 1 mol L<sup>-1</sup> H<sub>2</sub>SO<sub>4</sub>. Similar values were obtained for alkaline electrolyte (6 mol L<sup>-1</sup> KOH) with hydroquinone (275 F g<sup>-1</sup> at 5 mV s<sup>-1</sup>) being considerably higher than for electrolytes without dihydroxybenzenes. Such intriguing behaviour is closely related to electrochemical activity of these species, depending strongly on their stereochemistry and the electrolyte pH. The physicochemical investigations performed in order to confirm aforementioned assumptions, are in good accordance with such conclusion. The significant increase of the mass change recorded during TGA experiments (more than 15%) as well as the change in proton binding curves suggest that oxygen content in the electrode material increased. Some specific adsorption by  $\pi$  bonding of dihydroxybenzenes onto the carbon network cannot be excluded, however, the electrochemical results encourage us to assume that some part of these species were rather grafted on the carbon surface. Unfortunately, electrochemical reversibility of hydroquinones is not very high (ca. 60 %), thus the practical application of this redox couple is rather doubtful. On the other hand, capacitance retention was good during 5000 cycles with a subsequent gradual decrease. An interesting capacitance behaviour has been shown for bromodihydroxybenzene used as additive in alkaline medium (2 mol L<sup>-1</sup> solution). A great capacitance enhancement was observed because of bromide substitution in benzene ring. The significant increase of capacitance (50%) was found. Generally, a low regime was preferable for an efficient capacitor performance. The most beneficial results were obtained for alkali iodide, playing a dual role of electrolyte and redox active species simultaneously. The great advantage of this system is extraordinary reversibility due to the formation of iodine, in turn, polyiodides (I<sub>3</sub><sup>-</sup>, I<sub>5</sub><sup>-</sup>). Even if the high reversibility of I<sub>2</sub>/I<sub>n</sub><sup>-</sup> was observed in the narrow range of potential (below 200 mV) it greatly affected the total system. Electrochemical studies by floating complemented by the detailed capacitance measurements by other techniques proved exceptional performance of the capacitor based on iodides. Well documented enhancement of capacitance during floating is surely originated from cumulative creation of I<sub>n</sub><sup>-</sup> species but ultimate formation of iodates IO<sub>3</sub><sup>-</sup> should not be excluded. Raman spectra recorded *in situ* during the potentiostatic polarization were a good proof of an existence of I<sub>n</sub><sup>-</sup> species as well as for C-I interactions. The great interest of the iodide electrolytic solution for the capacitor application is also because of a usage of a cheap stainless steel current collector.

## Notes and references

- <sup>90</sup> *Poznan University of Technology, Institute of Chemistry and Technical Electrochemistry, Piotrowo 3, 60965 Poznan, Poland. Fax: 48 665 39 71; Tel: 48 665 36 32; E-mail: elzbieta.frackowiak@put.poznan.pl*
- <sup>95</sup> E. Frackowiak, F. Béguin *Carbon*, 2002, **40**, 1775
- Carbons for Electrochemical Energy Storage and Conversion Systems*, Ed. F. Béguin, E. Frackowiak, CRS Press Taylor&Francis Group, Boca Raton, 2010
- E. Frackowiak *Phys. Chem. Chem. Phys.* 2007, **9**, 1774

- 4 *Supercapacitors. Materials, systems and Applications*, Ed. F. Béguin, E. Frackowiak, Wiley-VCH Verlag GmbH&Co., Weinheim, 2013
- 5 J. Zhang, X.S. Zhao *ChemSusChem* 2012, **5**, 818
- 6 S. Suematsu, K. Naoi *J. Power. Sourc.* 2001, **97**, 816
- 7 Y.J. Oh, J.J. Yoo, Y.I. Kim, J.K. Yoon, H.N. Yoon, J.H. Kim, S.B. Park *Electrochim. Acta* 2014, **116**, 118
- 8 A. Yoshida, I. Tanahashi, A. Nishino *Carbon* 1990, **28**, 611
- 9 C.T. Hsieh, H. Teng *Carbon* 2002, **40**, 667
- 10 K. Okajima, K. Ohta, M. Sudoh *Electrochim. Acta* 2005, **50**, 2227
- 11 H.A. Andreas, B.E. Conway *Electrochim. Acta* 2006, **51**, 6510
- 12 E. Frackowiak, K. Fic, M. Meller, G. Lota *ChemSusChem* 2012, **5**, 1181
- 13 K. Fic, E. Frackowiak, F. Béguin *J. Mater. Chem.* 2012, **22**, 24213
- 14 S.T. Senthilkumar, R.K. Selvan, N. Ponpandian, J.S. Melo *RSC Advances* 2012, **2**, 8937
- 15 S.T. Senthilkumar, R.K. Selvan, Y.S. Lee, J.S. Melo *J. Mater. Chem. A* 2013, **1**, 1086
- 16 G. Lota, E. Frackowiak *Electrochem. Comm.* 2009, **11**, 87
- 17 G. Lota, K. Fic, E. Frackowiak *Electrochem. Comm.* 2011, **13**, 38
- 18 J. Menzel, K. Fic, M. Meller, E. Frackowiak *J. Appl. Electrochem.* 2014, **44**, 439
- 19 S. Yamazaki, T. Ito, M. Yamagata, M. Ishikawa *Electrochim. Acta* 2012, **86**, 294
- 20 P. Barpanda, G. Fanchini, G.G. Amatucci, *Electrochim. Acta* 2007, **52**, 7136
- 21 P. Barpanda, G. Fanchini, G.G. Amatucci, *Carbon* 2011, **49**, 2538
- 22 P. Barpanda, Y. Li, F. Cosandey, S. Rangan, R. Bartynski, G.G. Amatucci, *J. Electrochem. Soc.* 2009, **156**, A873
- 23 S. Roldan, M. Granda, R. Menendez, R. Santamaria, C. Blanco *J. Phys. Chem.* 2011, **115**, 17606
- 24 S. Roldan, C. Blanco, M. Granda, R. Menendez, R. Santamaria *Angew. Chem.* 2011, **123**, 1737
- 25 S. Isikli, R. Diaz *J. Power. Sourc.* 2012, **206**, 53
- 26 S. Isikli, M. Lecea, M. Ribagorda, M.C. Carreno, R. Diaz *Carbon* 2014, **66**, 654
- 27 G. Pognon, T. Brousse, L. Demarconnay, D. Bélanger *J. Power Sourc.* 2011, **196**, 4117
- 28 G. Pognon, T. Brousse, D. Bélanger *Carbon* 2011, **49**, 1340
- 29 D.M. Anjos, J.K. McDonough, E. Perre, G.M. Brown, S.H. Overbury, Y. Gogotsi, V. Presser *Nano Energy* 2013, **2**, 702
- 30 Z. Algharaibeh, P.G. Pickup *Electrochem. Commun.* 2011, **13**, 147
- 31 D. Bélanger, J. Pinson *Chem. Soc. Rev.* 2011, **40**, 3995
- 32 P.S. Guin, S. Das, P.C. Mandal *Int. J. Electrochem.* 2011, ID 816202
- 33 G. Lota, T.A. Centeno, E. Frackowiak, F. Stoeckli *Electrochim. Acta*, 2008, **53**, 2210
- 34 M. Mizuno, J. Tanaka, I. Harada *J. Phys. Chem.* 1981, **50**, 1789
- 35 E.M. Nour, L.H. Chen, J. Laane *J. Phys. Chem.* 1986, **90**, 2841
- 36 T.J. Marks, D.W. Kalina, *Extended Linear Chain Compounds*, Ed. J.S. Miller, Plenum (New York) 1982, **1**, 197
- 37 A.J. Blake, F.A. Devillanova, R.O. Gould, W.S. Li, V. Lippolis, S. Parsons, C. Radek, M. Schroder *Chem. Soc. Rev.* 1998, **27**, 195